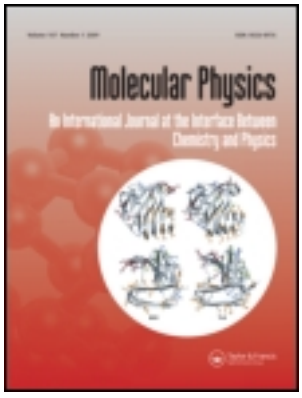

Molecular Physics: An International Journal at the Interface Between Chemistry and Physics
Publication details, including instructions for authors and subscription information:
http://www.tandfonline.com/loi/tmph20

Raman and IR spectroscopy research on hydrogen bonding in water-ethanol systems

Sergey Burikov [a], Tatiana Dolenko [a], Svetlana Patsaeva [a], Yuriy Starokurov [a] & Viktor Yuzhakov [a]

[a] Department of Physics, M.V. Lomonosov Moscow State University, Moscow 119991, Russia

Version of record first published: 30 Sep 2010.

To cite this article: Sergey Burikov , Tatiana Dolenko , Svetlana Patsaeva , Yuriy Starokurov & Viktor Yuzhakov (2010): Raman and IR spectroscopy research on hydrogen bonding in water-ethanol systems, Molecular Physics: An International Journal at the Interface Between Chemistry and Physics, 108:18, 2427-2436

To link to this article: http://dx.doi.org/10.1080/00268976.2010.516277

Molecular Physics
Vol. 108, No. 18, 20 September 2010, 2427–2436

Taylor & Francis
Taylor & Francis Group

INVITED ARTICLE

Raman and IR spectroscopy research on hydrogen bonding in water–ethanol systems

Sergey Burikov, Tatiana Dolenko, Svetlana Patsaeva*, Yuriy Starokurov and Viktor Yuzhakov

Department of Physics, M.V. Lomonosov Moscow State University, Moscow 119991, Russia

(*Received 30 January 2010; final version received 11 August 2010*)

Vibrational spectroscopy provides invaluable information about hydrogen bonding in aqueous solutions. To study changes in H-bonding due to increase of ethanol concentration in water, we perform research on water–ethanol binary mixtures with various mixing ratios using a combination of Raman scattering and IR absorption techniques. We study Raman spectra from 200 to 4000 cm^{-1} excited at 488 nm and IR spectra from 500 and 4000 cm^{-1} for solutions with different ethanol concentrations from pure water to pure ethanol. Using the intensity ratio of OH stretching band taken at 3200 and 3420 cm^{-1} for Raman spectra and at 3240 and 3360 cm^{-1} for IR spectra we evaluate the strength of H-bonding. Maximal strength of H-bonding in water–ethanol mixture corresponds to ethanol concentration 15–20% w/w. We explain it by the presence of transient ethanol hydrates similar in composition to gaseous clathrates with stoichiometric water/ethanol ratio 5:1. Further weakening of H-bonding with ethanol concentration is caused by the formation of chain aggregates from ethanol/water molecules. In addition, we apply other approaches, such as multivariate curve resolution-alternating least squares analysis, decomposition of water Raman stretching band, and comparison of water Raman stretching band in ethanol solutions to that of gas clathrates to support this hypothesis.

Keywords: Raman scattering; IR absorption spectra; stretching vibrations; hydrogen bonding; ethanol hydrates

1. Introduction

Detailed study of water–ethanol system for the first time was conducted by Russian chemist Dmitriy Mendeleev. In his Doctoral thesis (1865) 'Discourse on Alcohol and Water Mixing' [1], Mendeleev suggested a hypothesis that the following three compounds are formed in aqueous ethanol solutions: 'twelve-water alcohol' $Et{\cdot}12H_2O$, 'three-water alcohol' $Et{\cdot}3H_2O$, and compound of the composition $3Et{\cdot}H_2O$. Contrary to the view on solutions as simple 'mechanical' mixtures prevailing at that time, Mendeleev developed a theory of hydration based on the idea that mixing of different components in solutions results in the formation of new *compounds* (hydrates in modern terminology).

Numerous studies on water–alcohol systems reveal that such solutions are non-ideal, and this has been interpreted in terms of alcohol hydrates or a clathrate (like) structure formation [2–7]. Clathrate hydrate research is attracting attention anew because of increasing interest in clathrate chemistry [8], examination of clathrate hydrates as a possible energy resource [9] and their astrophysical implications [10,11]. Clathrate hydrate studies are also important in assessing geohazards to deep-water exploration and development [12]. It is worth mentioning that although the terms 'clathrate (like)' or 'quasi-clathrate' structure have long been used in scientific papers for description of water structure in aqueous solutions (see, e.g. [13–18]), there is no consensus among scientists on accepting the clathrate model in solutions [19–21].

In [2], it was proposed that water molecules surrounding *tert*-butanol molecules form a clathrate-like structure by hydrogen-bonded network and stabilize the cluster. This effect is usually called the 'hydrophobic hydration'. The evidence for the existence of clathrate hydrates in a number of alcohols is provided using dielectric relaxation technique and differential scanning calorimetry (DSC) [3], the stoichiometric ratio for clathrates is suggested to be around five to six water molecules per one alcohol molecule. X-ray diffraction measurements over a range from ambient to freezing point temperatures have been made on methanol–water, ethanol–water and 2-propanol–water mixtures, whose compositions are around mole fractions of the structural transition of solvent clusters at 25°C, i.e. ~0.3, ~0.2 and ~0.1, respectively [4]. The results show that the structure of dominant clusters formed in the mixtures at 25°C is still kept at low temperatures, except that H-bonds

*Corresponding author. Email: spatsaeva@mail.ru

ISSN 0026–8976 print/ISSN 1362–3028 online

DOI: 10.1080/00268976.2010.516277
http://www.informaworld.com

formed in the mixtures are gradually ordered with lowering temperature. At freezing point temperatures in methanol–water and ethanol–water mixtures ice, I_h is crystallised below the mole fraction of structural transition. Above the mole fraction of structural transition, methanol–water mixtures are kept in the metastable liquid state, but ethanol hydrate is crystallised in ethanol–water mixtures. It was concluded that the structure of dominant clusters formed in the mixtures at the ambient temperature is reflected into that of frozen alcohol–water mixtures.

The structure and composition of alcohol hydrates remained controversial even for water–ethanol systems better studied in the solid phase. The ethanol hydrate with a composition $Et{\cdot}5.67H_2O$ was found using DSC technique [5]. Two kinds of ethanol hydrates in water–ethanol systems were confirmed [6]: $Et{\cdot}4.67H_2O$ in solutions frozen just after mixing ethanol with water, and $Et{\cdot}4.75H_2O$ in solutions frozen after their storage for a few days at room temperature. In [7], using DSC technique, three ethanol hydrates in water–ethanol systems were found: $Et{\cdot}2H_2O$, $Et{\cdot}3H_2O$ and $Et{\cdot}4.75H_2O$. The last one is described as a semi-clathrate, i.e. clathrate in which the ethanol hydroxyl group is linked by H-bond to the surrounding water framework.

There are also other conceptions of water–ethanol mixtures. The low frequency Raman spectra of the ethanol–water binary solutions with various mixing ratios were found to be decomposed into linear combinations of the spectra of pure water and pure ethanol [22]. According to the results [22], water and ethanol do not get ideally mixed in the molecular level and the H-bonds between water associates and ethanol associates are weak; so, the authors propose a double-layer sandwich cluster model of ethanol molecules, which is stacked by hydrophobic interaction.

Hydrogen bonding plays a key role in the structural, physical and chemical properties of liquids, such as water, alcohols and in macromolecular structures like proteins. A water molecule can form up to four H-bonds (two donor and two acceptor bonds) in an approximately tetrahedral arrangement [23]. These H-bonds are continually being broken, and new bonds are being formed on a picoseconds time scale [24]. H-bonding plays an essential role in forming the structure of water–ethanol solutions [25–27]. A molecule of ethanol can form not more than two H-bonds (one donor and one acceptor). Water and ethanol molecules can also interact *via* H-bonding. The nature of molecular association in ethanol–water solutions is essential to understanding the structural basis of the physical and chemical properties of alcohol solutions. Despite decades of research on alcohol hydration, the understanding of structure of alcohol solutions is still incomplete [28,29].

Vibrational spectroscopy is an important tool for understanding H-bonding in water and aqueous solutions [23,30,31]. All transformations in vibrational spectra of water can be explained taking into consideration continuum of hydrogen-bonding states [32–36]. In a continuum model, liquid water comprises a random, three-dimensional network of hydrogen bonds with a broad distribution of distances and angles between hydroxyl groups of neighbouring molecules [37]. In the previous study of aqueous ethanol solutions by Raman scattering, we observed the transformations of non-homogeneously broadened OH stretching band with the increase of ethanol concentration and interpreted them in terms of hydrogen bonds strengthening at certain ethanol concentration [38]. Research group [39] analysed infrared (IR) spectra obtained for ethanol–water solutions applying the multivariate curve resolution-alternating least squares (MCR-ALS) method, and interpreted it using chemical shift behaviour in the NMR spectra. The results showed that these mixtures could be described by a mixture model consisting of four species: ethanol, water and two hydrates with water/ethanol ratios about 5:1 and 1:1.

In this study, we investigated water–ethanol mixtures with various mixing ratios ranging from pure water to pure ethanol, using a combination of Raman scattering and IR absorption spectroscopy. The contour analysis of a non-homogeneously broadened OH stretching band revealed changes in hydrogen bonding in solutions along with increasing ethanol concentration. In addition, we used the results of the MCR-ALS method [40] and decomposition of water Raman stretching band with a combination of optimization methods [41] to confirm our conclusions.

2. Experiment

Water–ethanol solutions were prepared from purified ethyl alcohol and bi-distilled water. The purity of alcohol and water was controlled by monitoring the absence of fluorescence excited by ultraviolet (UV) light. The ethanol concentration in the prepared solutions was changed from 0% to pure ethanol with 2–5% w/w step, and further it is expressed in weight percentages. We applied Raman measurements for all prepared solutions, while using IR measurements for solutions with 10% w/w increment in concentration.

2.1. *Raman measurements*

Raman spectra were excited using Ar-laser radiation (wavelength 488 nm, power 450 mW) and registered by means of a CCD camera with spectral resolution of $2\,cm^{-1}$. The Raman spectrometer is described in detail in [41]. The temperature of the samples was maintained constant and equal to $(22.0 \pm 0.2)^{\circ}C$. The spectra were corrected for the laser radiation power and acquisition time. Further data processing within the region of CH and OH stretching bands included normalizing spectra to the integrated intensity of both CH and OH bands.

2.2. *IR absorption measurements*

Fourier transform infrared-attenuated total reflectance (FTIR-ATR) spectroscopy of the aqueous ethanol solutions was carried out on a Varian 3100 FT-IR spectrometer (Varian Inc., Palo Alto, CA) equipped with a KRS-5 (a eutectic mixture of thallium and bromide iodides) internal reflection element. Liquid samples (0.1 mL) were placed directly on a total reflectance accessory. IR spectra were recorded between 500 and $4000\,cm^{-1}$ at a resolution of $1\,cm^{-1}$ using data collection software Varian Resolutions Pro v4.05, Varian Inc. To improve the signal to noise ratio, 100 scans were averaged for each spectrum. IR data were used without any data processing.

3. Spectral lines in Raman and IR spectra in water–ethanol solutions

Figure 1 shows Raman scattering spectra measured for water and aqueous ethanol solutions with different ethanol concentrations within wavenumber range $200–4000\,cm^{-1}$. Attribution of lines is given in the Table 1 according to [22,42–45]. The first number in the column displaying wavenumbers corresponds to diluted solution (<10% w/w) and the last one to 90% w/w ethanol. The last column represents our results on changes in Raman lines position measured from diluted solutions to concentrated ethanol. As it follows from Figure 1 and Table 1, along with the rising of ethanol concentration, the position and width of ethanol lines in Raman spectra are practically constant, while their amplitudes are increasing. Amplitudes of water bending and OH stretching bands are monotonously decreasing with rise of ethanol concentration in the solution. For Raman bands of stretching vibrations of CH- and OH-groups, besides the changes in intensity we observed remarkable changes in the spectral contour shape.

Similar changes were observed in the IR spectra of water–ethanol solutions with increasing mixing ratio.

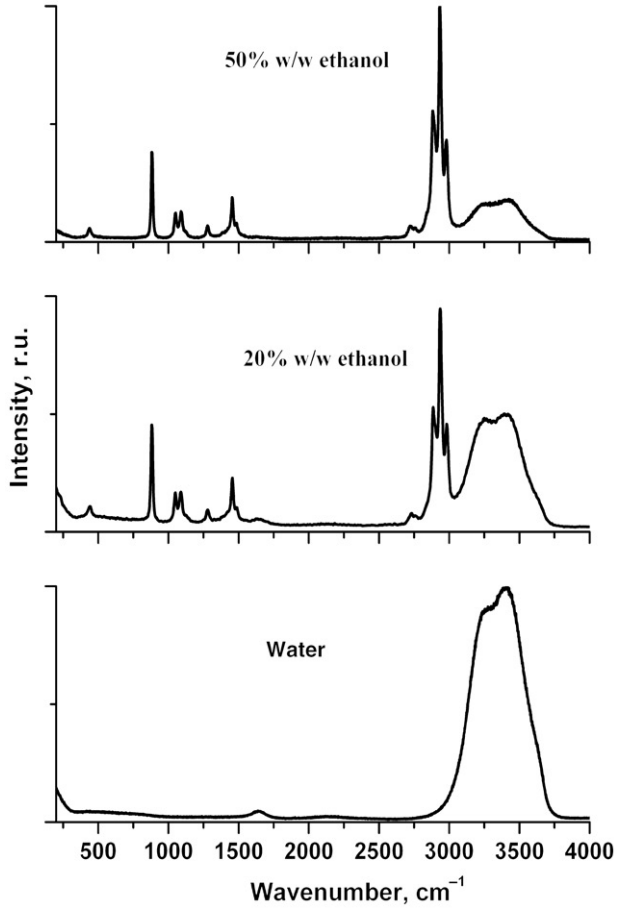

Figure 1. Raman scattering spectra of water and ethanol solutions within wavenumber range $200–4000\,cm^{-1}$.

Figure 2 presents the IR spectra measured for the same solutions as given in Figure 1.

4. OH stretching band in Raman and IR spectra of water–ethanol solutions

We devote special attention to behaviour of the OH stretching band in water–ethanol solutions due to the fact that the contour of this band is essentially affected by hydrogen bonding.

Figure 3 presents Raman spectra of water and ethanol solutions in the wavenumber region $2600–3800\,cm^{-1}$. Figure 4 demonstrates IR absorption spectra of water–ethanol solutions in the same wavenumber region. In both figures, the stretching lines of CH-groups apparently seen in the region $2800–3000\,cm^{-1}$ overlay the extremely wide and non-homogeneously broadened band of OH-groups of ethanol and water molecules spreading from 2900 to $3800\,cm^{-1}$. Upon increasing ethanol concentration

Table 1. Characteristics of Raman lines in the wavenumber range 200–4000 cm^{-1} for aqueous ethanol solutions. In the column with wavenumbers, the first number corresponds to diluted solution (<10% w/w) and the last one to 90% w/w ethanol.

$\Delta\nu$ (cm^{-1})	Raman line assignment	Line position changes in Raman spectra measured from diluted solutions to pure ethanol
440	Bending vibrations of C–C–O	No changes in position
886	Stretching vibrations C–C	No changes in position
1056	Stretching vibrations C–O	No changes in position
1100–1116	Librations, rock vibrations CH_3	Blue shift in 6 cm^{-1}
1280	Torsion and rotational vibrations CH_2	No changes in position
1456	Bending vibrations of CH_3 and CH_2	No changes in position
1486	Bending vibrations of CH_3	No changes in position
1630	Bending vibrations of water	No changes in position, the band is very weak at ethanol concentration ≥35% w/w
2730–2721	Combinational frequencies	Red shift in 9 cm^{-1}
2764	Combinational frequencies	No changes in position
2884	Stretching symmetric vibrations CH_2	Very small maximum shift
2932	Stretching symmetric vibrations CH_3	Very small maximum shift
2985–2977	Stretching asymmetric vibrations CH_3	Starting from ethanol concentration 15% w/w shifts in 8 cm^{-1} to lower frequencies
3400 ± 4–3330 ± 20	Stretching vibrations of OH-groups	No changes in position till ethanol concentration 90% w/w, but then it remarkably shifts to lower wavenumbers

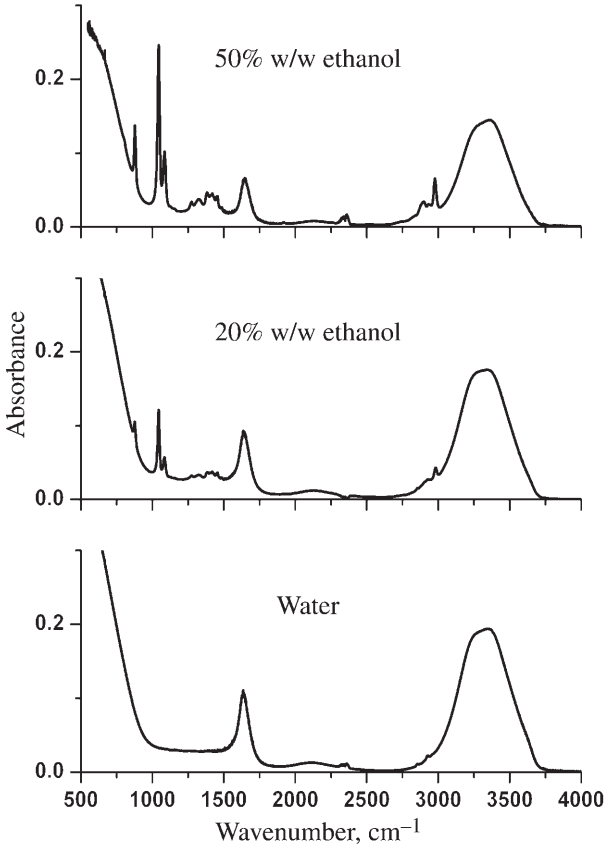

Figure 2. IR absorption spectra of water and ethanol solutions within wavenumber range 500–4000 cm^{-1}. Ethanol concentrations are the same as in Figure 1.

in the solution, the OH band undergoes changes not only in its integral intensity, but also in the contour shape and the ratio of intensities taken at low-frequency (around 3200 cm^{-1}) to high-frequency (around band maximum) regions.

4.1. *Intensity ratio for OH stretching band*

To quantify changes in spectral contour shape for OH band, we took the amplitude ratio at vibration frequencies of OH-groups linked with strong and weak H-bonds [30,31]. To characterise changes in the Raman spectra, we measured the ratio of Raman intensities at 3200 and 3420 cm^{-1}. For IR spectra, we took the ratio of absorbance values at 3240 and 3360 cm^{-1}. The ratio values as a function of ethanol concentration for Raman spectra and IR spectra are shown in Figures 5 and 6, respectively. Both graphs demonstrate that the ratio goes through a maximum around an ethanol concentration of 10–20% w/w. We interpret these results in terms of strengthening hydrogen bonding in the solution at certain ethanol concentrations. It should not be regarded as proof of the fact that the ethanol solution is more water-like than pure water. Our data show only that hydrogen bonding between water molecules at certain ethanol concentrations is higher compared to that in pure water.

To support this conclusion, we performed decomposition of water Raman stretching band into Gaussian-shape components for water–ethanol binary mixtures of various ethanol concentrations [41].

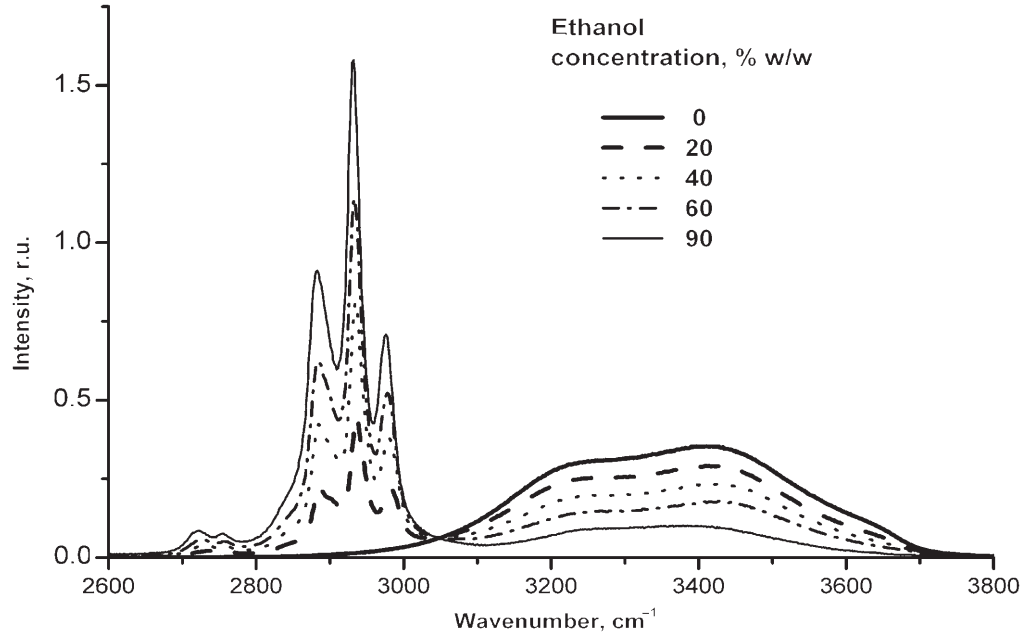

Figure 3. Raman scattering spectra of water and ethanol solutions with various ethanol concentrations within the region of CH and OH stretching bands.

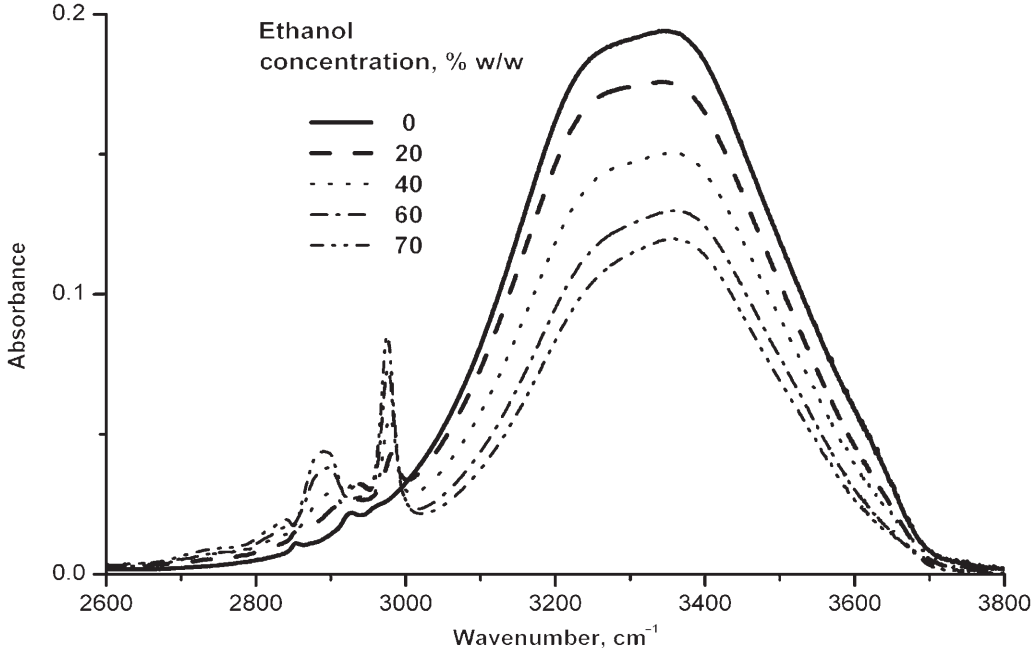

Figure 4. IR absorption spectra of water and ethanol solutions with various ethanol concentrations within the region of CH and OH stretching bands.

Deconvolution of the OH stretching band revealed three main spectral components' with maxima located around 3200 (vibrations of strongly H-bonded OH-groups), 3450 (weakly H-bonded OH-groups) and 3650 cm^{-1} (vibrations of free OH-groups without H-bonding). The behaviour of components' parameters as a function of ethanol concentration was studied using a combination of genetic algorithm and the

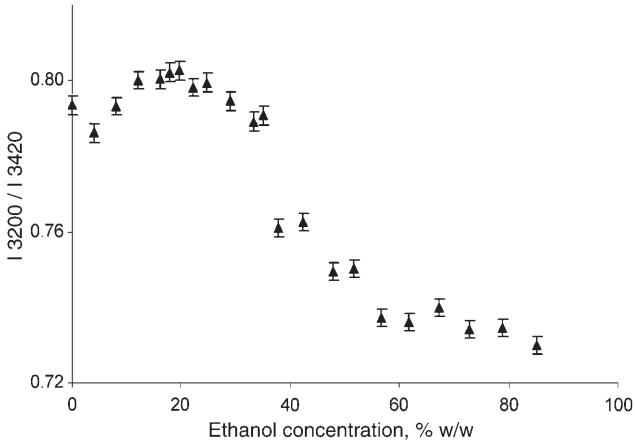

Figure 5. Ratio of Raman intensities taken at wavenumbers 3200 and 3420 cm^{-1} as a function of ethanol concentration in solution.

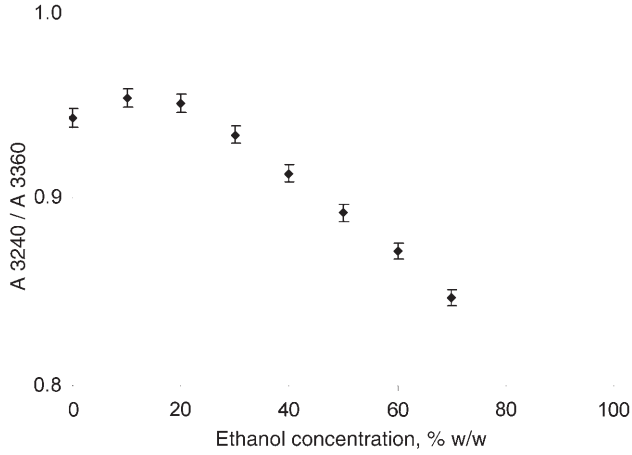

Figure 6. Ratio of absorbance values taken at wavenumbers 3240 and 3360 cm^{-1} as a function of ethanol concentration in solution.

generalized reduced gradient method. The analysis showed that in certain range of alcohol concentrations, one can observe non-monotonous behaviour of the position, width and intensity ratios of main spectral components in OH stretching band. Noticeable changes in band parameters for vibrations of strongly H-bonded OH-groups start to occur at concentration values around 22–24% by volume, which corresponds to 18–20% of weight. We explain such abnormal behaviour by H-bond strengthening resulting from structural rearrangements in the solutions at the specified concentrations of alcohol.

4.2. *MCR-ALS component analysis of CH and OH stretching bands*

MCR-ALS analysis [46,47] is a chemometric method, and recently it has been used to study a molecular association in alcohol solutions [48,49]. Three-component and four-component MCR-ALS analysis has been used to resolve the Raman and IR spectra which are composed of overlapping bands and to identify the composition of methanol hydrates [48]. The results allow us to apply a mixture model to describe the structure of water–methanol mixtures. The model consists of four species, namely, methanol, water and two complexes, methanol/water (1:1) and methanol/water (1:4). In [49], the composition of a 1-propanol hydrate (1:1) was reported based on a three-component factor analysis of mid-IR attenuated total reflection (mid-IR-ATR) spectra.

In [39,40], MCR-ALS analysis was applied to IR spectra of water–ethanol solutions with the aim to investigate the structure of these binary mixtures. A mixture model consisting of ethanol, water and two hydrates, water-rich and ethanol-rich, proved adequate to describe concentration dependencies of water–ethanol systems. Concentration profiles of resolved components were determined; and the maximum concentration of water-rich hydrate in aqueous ethanol solutions was observed to correspond to ethanol fraction ~0.1 (that is ~22% w/w). This result agrees well with other experimental data [50–52], which by using optical spectroscopy show that ethanol stabilizes the structure of aqueous solution at a concentration close to 20% w/w.

4.3. *Water/ethanol ratio estimation in ethanol hydrates*

The MCR-resolved components were identified in [39] by comparing the resolved spectrum to the closest IR spectrum of ethanol solutions. The composition of ethanol hydrates was determined as $EtOH \cdot 5.4H_2O$ and $EtOH \cdot 1.3H_2O$. Another approach to determine the composition of ethanol–water hydrates from Raman and IR spectra was used in [40]. We calculated the integrated intensities of CH or OH band, and divided each value by their sum area, consequently, $I_{CH}/(I_{CH}+I_{OH})$ and $I_{OH}/(I_{CH}+I_{OH})$, for vibrational spectra of ethanol solutions with known concentration as well as for MCR-resolved components. Then, we used the concentration dependency of either $I_{CH}/(I_{CH}+I_{OH})$ or $I_{OH}/(I_{CH}+I_{OH})$ to interpolate the water/ethanol ratio for MCR-resolved hydrates. Thus, we received the hydrate numbers of the resolved components for water-rich hydrate (5 (Raman) and 4.3 (mid-IR)), and for the second hydrate (1 (Raman)

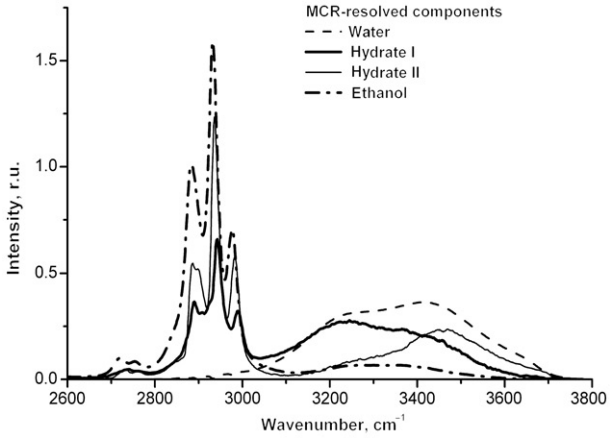

Figure 7. MCR-ALS resolved components in Raman spectra of aqueous ethanol solutions with various ethanol concentrations.

and 2.4 (mid-IR)). We came to the conclusion that the composition of the water-rich hydrate (hydrate I) is close to $EtOH \cdot 5H_2O$, and the ratio for another hydrate (hydrate II) water/ethanol lies between 1 and 2.

4.4. *The shape of MCR-resolved spectral contours*

In this study, the results of application of MCR-ALS method to the Raman CH and OH stretching bands in water–ethanol mixtures were used to analyse the shape of resolved spectral components. Although the MCR-ALS method is not a technique for direct spectral deconvolution, its application can reveal changes in intensities for different types of stretching CH and OH vibrations along with rising ethanol concentration. The resolved spectra are shown in Figure 7 for four components: water, two types of ethanol hydrate and ethanol. Two of them are almost identical to Raman scattering spectra of pure water and pure ethanol. However, other two spectra of ethanol hydrates resolved by MCR-ALS differ in shape from the Raman scattering spectra of aqueous ethanol solutions. The spectrum for hydrate I in Figure 7 shows a higher ratio of intensities taken at low-frequency ($\sim 3200\,cm^{-1}$) and high-frequency (around band maximum) regions, compared to that of water (see also Figure 3). If we take into consideration that the low-frequency region corresponds to vibrations of strongly H-bonded OH-groups, and the region around $3450\,cm^{-1}$ is caused by vibrations of weakly H-bonded OH-groups, we conclude that hydrogen bonding between water molecules in water-rich hydrate has strengthened compared to that of pure water.

One may also notice that the shape of OH stretching band in the resolved water-rich hydrate resembles the bandshape of water Raman spectrum for a solid gas clathrate of structure II [53] presented in Figure 8. In both cases, hydrogen bonding between water molecules is reinforced due to restructuring of water framework surrounding the 'guest' compound: either the methane molecule or the hydrophobic part of the ethanol molecule.

In contrast to hydrate I, from the shape of resolved spectrum for another ethanol hydrate (hydrate II in Figure 7) we conclude that H-bonding between hydroxyl groups in this structure is weaker than in pure water. This type of ethanol hydrates most likely represents zigzag water–ethanol chain associates, where water molecules are not able to form four H-bonds. With ethanol concentration exceeding 20% w/w in solution, the number of such ethanol hydrates is rising followed by weakening of hydrogen bonding in solution. Consequently, continuous decrease in intensity ratio (both in Raman and IR spectra) taken at low-frequency and high-frequency regions has been observed (Figures 5 and 6). This result is consistent with the changes in H-bond structure revealed by absorption and fluorescence emission spectroscopy: tetrahedral network transforms into zigzag chains with increasing ethanol concentration in water [54].

5. Discussion of results

Modern conceptions of water structure [15,16,55–57] and the theory of hydrophobic hydration provide a basis for interpretation of our research results (experimental data) [58–61]. The maxima/minima in many physical properties suggest a fundamental structural change which depends on the hydrophobe/hydrophil group ratio [15]. Adding a small amount of non-polar solute to water leads to anomalous characteristics of the hydrophobic effect due to rearrangements in hydrogen bonding. For instance, adding a small quantity of alcohol to water makes the viscosity of the mixture higher than that of each of the components [56,62]. The molecular-jump reorientations of water molecules are gradually slowing down [63] or switched off [64] near hydrophobic groups. At ethanol concentration around 15% w/w in water, there are enough alcohol molecules to destroy the H-bond network typical for liquid water, and to form a new type of H-bond organization. Remarkable changes in the shape of OH stretching band due to hydrogen bonding of hydroxyl groups in ethanol and water molecules occur in Raman spectra. Maximal strength of H-bonds in water–ethanol mixture corresponds to ethanol

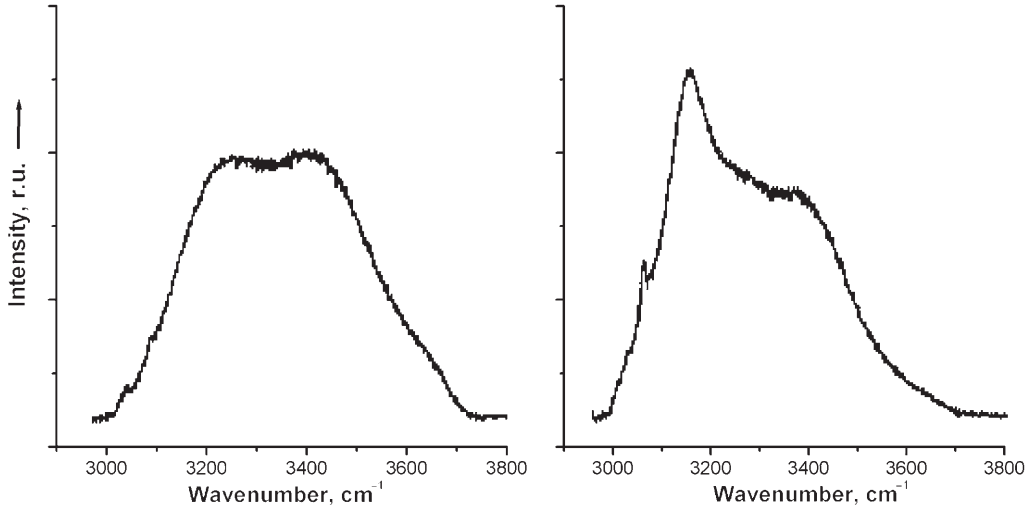

Figure 8. Raman scattering spectra in methane hydrates of structure II (left) and structure I (right) within the region of OH stretching band (adopted from [37]).

concentration 15–20% w/w. We attribute this structure of water molecules with enhanced H-bonding in presence of ethanol to a specific type of ethanol hydrate.

Application of MCR-ALS analysis to Raman spectra of water–ethanol solutions gave us four MCR-resolved components contributing into spectral concentration dependences: water molecular aggregates, ethanol aggregates and two types of ethanol hydrates. First of these ethanol hydrates is similar in composition to clathrates with stoichiometric ratio 5:1 of water and guest molecules. Hydrogen bonding in water-rich hydrate is stronger than that of pure water due to rearrangement of H-bonds between water molecules surrounding ethanol molecule. The hydrogen bonds between water molecules are continually breaking and reforming, producing, on average, distorted clathrate-like organization. The size of water-rich hydrate with composition $EtOH \cdot 5H_2O$ is not limited to six molecules; contrariwise, such a structure involves large ensemble of water and ethanol molecules with their molecular ratio 5:1.

With increasing ethanol concentration, water molecules cannot produce completed H-bonds with neighbouring liquids; so, clathrate-like structures are destroyed and gradually replaced by zigzag chains formed from ethanol and water molecules with stoichiometric ratio ranging from 2 to 1. Formation of ethanol hydrate of chain structure causes further weakening of H-bonding with increased ethanol concentration.

Hydrophobic interaction and clathrate-like structures in solutions attract attention of researchers nowadays and present particular interest for further studies.

6. Conclusions

The results presented in this article prove that essential structural rearrangement occur in water–ethanol solutions. Behaviour of OH stretching band in Raman and IR spectra with increasing ethanol concentration showed that hydrogen bonding in solutions at ethanol concentration around 15–20% w/w is stronger compared to that of pure water. At concentrations exceeding 20% w/w, the strengthening of hydrogen bonding is gradually decreasing towards concentrated ethanol solutions. MCR-ALS component analysis revealed four components that make main contributions to concentration dependences in vibrational spectra of water–ethanol solutions: pure water, water-rich hydrate $EtOH \cdot 5H_2O$, ethanol-rich hydrate $EtOH \cdot 1H_2O \div EtOH \cdot 2H_2O$ and pure ethanol. The increased intensity around 3200 cm^{-1} in the contour of MCR-resolved component (namely, water-rich hydrates) also confirms that H-bonding in this hydrate is stronger than in pure water. Besides, the lineshape of OH stretching band in the MCR-resolved spectrum of water-rich hydrate resembles water stretching band in Raman spectrum of a solid gas clathrate [53]. Hydrate stoichiometric ratio and strengthening of H-bonds between its water molecules corroborate its clathrate-like organization. By this term, we mean the transient structure formed around ethyl groups by water molecules with H-bonds continuously breaking and reforming.

Acknowledgements

The authors thank Prof. Dale W. Schaefer and Dr Naiping Hu, Department of Chemical and Materials Engineering, University of Cincinnati, USA for performing MCR-ALS analysis and for helpful discussion of results.

References

[1] D.I. Mendeleev, *Discourse on Alcohol and Water Mixing*, published in the book *Solutions* (Akad. Nauk SSSR, Moscow, 1959), p. 381 (in Russian).
[2] K. Iwasaki and T. Fujiyama, J. Phys. Chem. **81** (20), 1908 (1977).
[3] S.S.N. Murthy, J. Phys. Chem. A **103**, 7927 (1999).
[4] T. Takamuku, K. Saisho, S. Nozawa and T. Yamaguchi, J. Mol. Liq. **119**, 133 (2005).
[5] K. Takaizumi and T. Wakabayashi, J. Solution Chem. **26**, 927 (1997).
[6] K. Takaizumi, J. Solution Chem. **34** (5), 597 (2005).
[7] Yu.M. Zelenin, Zh. Strukt. Khimii **44** (1), 155 (2003) (in Russian).
[8] Yu.A. Dyadin, I.S. Terekhova, T.V. Rodionova and D.V. Soldatov, Zh. Strukt. Khimii **40** (5), 645 (1999).
[9] K.C. Hester and P.G. Brewer, Annu. Rev. Mar. Sci. **1**, 303 (2009).
[10] D.P. Hand, C.F. Chyba, R.W. Carlson and J.F. Cooper, Astrobiology **6** (3), 463 (2006).
[11] D. Blake, L. Allamandola, S. Sanford, D. Hudgins and F. Freund, Science **254**, 548 (1991).
[12] D. Long, P.D. Jackson, M.A. Lovell, C.A. Rochelle, T.J.G. Francis and P.J. Schultheiss, Petroleum Geology Conference Series **6**, 723 (2005).
[13] G.E. Walrafen and Y.C. Chu, J. Phys. Chem. **99** (26), 10635 (1995).
[14] T. Head-Gordon, PNAS **92** (18), 8308 (1995).
[15] F. Franks, *Water: A Matrix of Life*, 2nd ed (The Royal Society of Chemistry, Cambridge, 2000).
[16] C. Reichardt, *Solvents and Solvent Effects in Organic Chemistry*, 3rd ed (Wiley-VCH Verlag GmbH & Co. KGaA, Weinheim, 2003).
[17] T. Yokono, S. Shimokawa, T. Mizuno, M. Yokono and T. Yokokawa, Jpn. J. Appl. Phys. **43** (11A), L1436 (2004).
[18] H. Yokoyama, M. Kannami and H. Kanno, Chem. Phys. Lett. **463** (1–3), 99 (2008).
[19] H. Ashbaugh, D. Asthagiri, L. Pratt and S. Rempe, Biophys. Chem. **105** (2–3), 323 (2003).
[20] A.K. Soper, L. Dougan, J. Crain and J.L. Finney, J. Phys. Chem. B **110** (8), 3472 (2006).
[21] T.P. Silverstein, J. Chem. Educ. **85** (7), 917 (2008).
[22] K. Egashira and N. Nishi, J. Phys. Chem. B **102**, 4054 (1998).
[23] D. Eisenberg and W. Kauzmann, *The Structure and Properties of Water* (Clarendon Press, Oxford, 1969).
[24] R.A. Nicodemus, K. Ramasesha, S.T. Roberts and A. Tokmakoff, J. Phys. Chem. Lett. **1** (7), 1068 (2010).
[25] K. Mizuno, Y. Miyashita, Y. Shindo and H. Ogawa, J. Phys. Chem. **99** (10), 3225 (1995).
[26] A. Nose and M. Hojo, J. Biosci. Bioeng. **102** (4), 269 (2006).
[27] A. Nose, M. Hojo and T. Ueda, J. Phys. Chem. B **108**, 198 (2004).
[28] J.J. Max, S. Daneault and C. Chapados, Can. J. Chem. **80** (1), 113 (2002).
[29] S. Dixit, J. Crain, W.C.K. Poon, J.L. Finney and A.K. Soper, Nature **416** (6883), 829 (2002).
[30] T.A. Gogolinskaya, S.V. Patsaeva and V.V. Fadeev, Dokl. Akad. Nauk **290** (5), 1099 (1986) [Sov. Phys. Dokl. **31** (5), 820 (1986)].
[31] S. Burikov, T. Dolenko, V. Fadeev and I. Vlasov, Laser Phys. **17** (9), 1 (2007).
[32] Yu.Ya. Efimov and Yu.I. Naberukhin, Mol. Phys. **101** (3), 459 (2003).
[33] Yu.Ya. Efimov and Yu.I. Naberukhin, Mol. Phys. **102** (13), 1407 (2004).
[34] P.L. Geissler, J. Am. Chem. Soc. **127** (42), 14930 (2005).
[35] J.D. Eaves, J.J. Loparo, C.J. Fecko, S.T. Roberts, A. Tokmakoff and P.L. Geissler, PNAS **102** (37), 13019 (2005).
[36] C.J. Fecko, J.D. Eaves, J.J. Loparo, A. Tokmakoff and P.L. Geissler, Science **301** (5640), 1698 (2003).
[37] J.D. Smith, C.D. Cappa, K.R. Wilson, R.C. Cohen, P.L. Geissler and R.J. Saykally, PNAS **102** (40), 14171 (2005).
[38] S.A. Burikov, T.A. Dolenko, S.V. Patsaeva and V.I. Yuzhakov, Atmos. Oceanic Opt. **22**, 1082 (2009).
[39] N. Hu, D. Wu, K. Cross and D.W. Schaefer, Appl. Spectrosc. **64** (3), 337 (2010).
[40] N. Hu, D. Wu, K. Cross, S. Burikov, T. Dolenko, S. Patsaeva and D.W. Schaefer, J. Agric. Food Chem. **58**, 7394 (2010).
[41] S. Burikov, S. Dolenko, T. Dolenko, S. Patsaeva and V. Yuzhakov, Mol. Phys. **108** (6), 739 (2010).
[42] Y. Yu, K. Lin, X. Zhou, H. Wang, S. Liu and X. Ma, J. Phys. Chem. **111** (25), 8971 (2007).
[43] J.F. Mammone, S.K. Sharma and M. Nicol, J. Phys. Chem. **84** (23), 3130 (1980).
[44] D. Cleveland, M. Carlson, E.D. Hudspeth, L.E. Quattrochi, K.L. Batchler, S.A. Balram, S. Hong and R.G. Michel, Spectrosc. Lett. **40** (6), 903 (2007).
[45] L.A. Kazitsyna and N.B. Kupletskaya, *Application of UV, IR and NMR Spectroscopy in Organic Chemistry* (Vysshaya Shkola, Moscow, 1971).
[46] R. Tauler and A. de Juan, Multivariate Curve Resolution-Alternating Least-Squares (MCR-ALS), MatLab code (University of Barcelona, Spain, 1999).
[47] J. Mendieta, M.S. DiazCruz, R. Tauler and M. Esteban, Anal. Biochem. **240** (1), 134 (1996).
[48] C.A. Holden, S.S. Hunnicutt, R. Sanchez-Ponce, J.M. Craig and S.C. Rutan, Appl. Spectrosc. **57** (5), 483 (2003).
[49] J.J. Max, S. Daneault and C. Chapados, Can. J. Chem. **80** (1), 113 (2002).

[50] D.V. Ageev, S.V. Patsaeva, B.D. Ryzhikov, V.N. Sorokin and V.I. Yuzhakov, Zh. Prikl. Spektrosk. **75** (5), 640 (2008) [J. Appl. Spectrosc. **75** (5), 653 (2008)].
[51] M.F. Vuks and L.V. Shurupova, Opt. Spektrosk. **40** (1), 154 (1976) (in Russian).
[52] L.V. Shurupova, Vestnik SPbGU **4** (25), 16 (1994) (in Russian).
[53] J.M. Schics, J. Erzinger and M.A. Zieman, Spectrochim. Acta. A **61** (10), 2399 (2005).
[54] T. Pradhan, P. Ghoshal and R. Biswas, J. Chem. Sci. **120** (2), 275 (2008).
[55] M. Chaplin, *Water Structure and Behavior* (2009). <http://www.lsbu.ac.uk/water>
[56] P.J. Kramer and J.S. Boyer, *Water Relations of Plants and Soils* (Academic Press, New York, 1995).
[57] G.N.I. Clark, C.D. Cappa, J.D. Smith, R.J. Saykally and T. Head-Gordon, Mol. Phys. **108** (11), 1415 (2010).
[58] M.N. Buslaev and O. Ya. Samoilov, Zh. Strukt. Khimii **4** (4), 502 (1963) (in Russian).
[59] V.I. Yashkichev and O.Ya. Samoilov, Zh. Strukt. Khimii **3** (2), 211 (1962) (in Russian).
[60] Z.I. Grigorovich and O. Ya. Samoilov, Zh. Strukt. Khimii **3** (4), 464 (1962) (in Russian).
[61] K.A. Dill, T.M. Truskett, V. Vlachy and B. Hribar-Lee, Annu. Rev. Biophys. Biomol. Struct. **34**, 173 (2005).
[62] M. Ageno and C. Frontali, PNAS **57** (4), 856 (1967).
[63] K. Yoshida, A. Kitajo and T. Yamaguchi, J. Mol. Liq. **125** (2–3), 15 (2006).
[64] A.A. Bakulin, C. Liang, T. la Cour Jansen, D.A. Wiersma, H.J. Bakker and M.S. Pshenichnikov, Acc. Chem. Res. **42** (9), 1229 (2009).